Available online at www.sciencedirect.com
SCIENCE DIRECT®
Journal of Catalysis 221 (2004) 594–600
JOURNAL OF CATALYSIS
www.elsevier.com/locate/jcat

Role of the state of the metal component on the light-off performance of Pd-based three-way catalysts

M. Fernández-García,[a,*] A. Iglesias-Juez,[a] A. Martínez-Arias,[a] A.B. Hungría,[a] J.A. Anderson,[b] J.C. Conesa,[a] and J. Soria [a]

[a] *Instituto de Catálisis y Petroleoquímica, CSIC, Campus Cantoblanco, 28049 Madrid, Spain*
[b] *Division of Physical and Inorganic Chemistry, University of Dundee, DD14HN, Scotland, UK*

Received 4 June 2003; revised 17 September 2003; accepted 25 September 2003

Abstract

The behavior of Pd-based systems supported on alumina and ceria–zirconia and the complex ceria–zirconia on alumina was investigated during light-off tests using a stoichiometric $C_3H_6 + CO + NO + O_2$ mixture. In situ XANES/DRIFTS studies of the Pd chemical state at the surface and bulk of the materials were conducted to determine the noble metal response to the gas atmosphere during light off. The initial, oxidized PdO-like phase was converted to Pd(0) in all cases except for the ceria–zirconia-supported catalyst. Contact between Pd and bulk ceria–zirconia particles appeared to stabilize Pd clusters in the 373–673 K region with an average Pd(I)-like oxidation state. The presence of hydrocarbon in the gas phase was essential in order to stabilize these Pd(I)-like species. The role of such a phase in providing a source of active oxygen for hydrocarbon oxidation is shown here to strongly decrease light off temperature and this, together with its stability over a wide range of temperatures, may offer a contribution to reducing hydrocarbon emissions during cold start.

Keywords: Pd; Ceria–zirconia; Alumina; TWCs; Light off; XANES; DRIFTS

1. Introduction

Three-way catalysts (TWC) have been widely used to diminish pollutant emissions from gasoline engine powered vehicles [1–3]. Classical components of these systems usually include Rh, Pt, and/or Pd as active metals, ceria as promoter, and high surface alumina as the support [1–3]. The use of Pd as the single active metal component in TWCs has recently received considerable attention as a result of the high cost and scarcity of Rh, the availability of cleaner fuels, and its remarkable activity for oxidation reactions [1,3,4]. The classical promotion by ceria has been enhanced by inclusion of other oxide components in order to increase or maintain the durability of the TWC while decreasing the pollutant produced during the cold-start (or light off) period, which may represent a considerable portion of the total emissions produced during any driving cycle [1,4]. Among the latter, fluorite-type materials and, in particular, Ce–Zr mixed oxide systems, have been considered as substitutes of ceria on the basis of their greater oxygen storage capacity (OSC) after thermal sintering, which could potentially decrease the cold-start emissions mainly by allowing the catalyst to be located in positions closer to the engine manifold with minimum system deactivation being produced [3,5]. Optimum promoter properties are achieved at Ce/Zr atomic ratios close to one and when pseudocubic (tetragonal symmetry for oxygen sublattice) or cubic structures of the mixed oxide are formed, which are presumably stabilized as nanosized particles [6–9].

Due to the complexity of the great variety of depollution chemical reactions involved in TWCs, a degree of controversy exists with respect to the most adequate configuration of the noble metal–support interaction in order to achieve optimum catalytic properties [3,4,10–12]. It is well known that limitations exist for Pd-only systems with respect to their performance for NO reduction reactions [4,10,11], which can be mostly resolved by careful engineering of the solid catalyst, allowing part of the Pd to interact with the bare alumina [3] or at the alumina interface with bidimensional patches of CZ [13]. However, in order to accomplish environmental limitations formulated by ultralow level (ULEV)

* Corresponding author.
E-mail address: m.fernandez@icp.csic.es (M. Fernández-García).

0021-9517/$ – see front matter
doi:10.1016/j.jcat.2003.09.022

or super ultralow level (SULEV) vehicles significant effort has been focused on the reduction of hydrocarbon (HC) in the exhaust [1,3]. The majority of HCs (60–80%) are produced during the cold-start period of the driving cycle and thus it would be most desiderable if a close-coupled technology could handle this problem [3]. Unlike CO and, probably, NO, HC conversion is typically not strongly promoted by oxygen-storage materials [3,14,15], but the presence of oxidized Pd species has been shown to provide a source of oxygen to effectively enhance light off during cold-start conditions [15,16]. The existence and maintenance of oxidized Pd species in TWC systems during a light-off run are therefore a question of practical interest which has received little attention in the literature of HC oxidation reactions [17–19]. In the present study, Pd-based systems using three different supports, alumina (A), ceria–zirconia (CZ), and ceria–zirconia/alumina (CZA), have been analyzed in order to gain some insight into the potentially important parameters involving the interaction of the noble metal and the support which may be responsible for stabilizing an appropriate oxidation state of Pd during a $C_3H_6 + CO + NO + O_2$ reaction run. As described elsewhere [3,19], Pd-based TWC systems evolve in a similar way under this model gas mixture than during engine tests in light-off experiments. The three supports, on the other hand, enable analysis of Pd behavior under the interaction with all main supporting phases existing in TWCs; namely, alumina and two- and three-dimensional patches of CZ [20]. In situ XANES was used to follow the Pd oxidation state and phase distribution throughout the light-off test while parallel in situ DRIFTS provided information concerning the surface state of the noble metal.

2. Experimental

A ceria–zirconia/alumina support with 10 wt% mixed oxide—expressed as $Ce_{0.5}Zr_{0.5}O_2$—was prepared by modification of the microemulsion method as used previously for preparing the unsupported ceria–zirconia oxide [6]. This method allows a precise control of the primary and secondary particle size; full details of the procedure and its influence in the physicochemical characteristics of the promoter phase can be found elsewhere [7]. After drying overnight at 373 K, these supports were calcined in air at 773 K for 2 h ($S_{BET} = 105$ (CZ) and 186 (CZA) $m^2\,g^{-1}$). According to ICP-AES chemical analysis, both ceria–zirconia materials have a Zr/Ce atomic ratio of 1.0 ± 0.1. The alumina, A, (Condea; $S_{BET} = 180\,m^2\,g^{-1}$), CZ, and CZA supports were impregnated (incipient wetness method) with aqueous solutions of palladium (II) nitrate (Alfa Caesar; purities > 99.99%) in an amount to give 1.0 wt% of the precious metal. The catalysts were calcined following the same drying/calcination procedure described above for the supports and are referred to as PdA, PdCZA, and PdCZ.

Catalytic tests using stoichiometric mixtures of 0.1% C_3H_6 + 1% CO + 0.9% O_2 + 0.1% NO (N_2 balance) at 30,000 h^{-1} were performed in a Pyrex glass flow reactor system. Details of the experimental conditions employed for these tests can be found elsewhere [20]. Gases were regulated with mass flow controllers and analyzed using an online Perkin-Elmer 1725X FTIR spectrometer coupled with a multiple reflection transmission cell (Infrared Analysis Inc.; 2.4 m path length). Oxygen concentrations were determined using a paramagnetic analyzer (Servomex 540A). Experimental error in the HC, CO, and/or NO conversion values obtained in these conditions is estimated as ±7%. Prior to catalytic testing, in situ calcination was performed in diluted oxygen (2.5% O_2 in N_2) at 773 K, followed by cooling under the same atmosphere and subsequent N_2 purging at room temperature (RT). A typical test consisted of increasing the temperature from 298 to 823 K at 5 K min^{-1}.

DRIFTS analysis of adsorbed species present on the catalyst surface under reaction conditions was carried out using a Perkin-Elmer 1750 FTIR fitted with an MCT detector. Analysis of the NO conversion at the outlet of the IR chamber was performed by chemiluminescence (Thermo Environmental Instruments 42C). Additional postcatalyst gas analysis was performed using a Baltzers Prisma Quadrupole mass spectrometer. The DRIFTS cell (Harrick) was fitted with CaF_2 windows and a heating cartridge that allowed samples to be heated to 773 K. Samples of ca. 80 mg were calcined in situ at 773 K (with synthetic air 20% O_2 in N_2) and then cooled to 298 K in synthetic air before the introduction of the reaction mixture and subsequent heating at 5 K min^{-1} up to 673 K, recording one spectrum (4 cm^{-1} resolution, average of 20 scans) generally every 10–15 K. The gas mixture (using the same concentrations as those employed for laboratory reactor tests) was prepared using a computer-controlled gas blender with 75 $cm^3\,min^{-1}$ passing through the catalyst bed.

XANES experiments at the Pd *K*-edge were performed on line BM29 of the ESRF synchrotron at Grenoble. A Si (311) double-crystal monochromator was used in conjunction with a rejection mirror to minimize the harmonic content of the beam. Transmission experiments were carried out using Kr/Ar-filled ionization chambers. The energy scale was simultaneously calibrated by measuring the corresponding metal foil inserted before a third ionization chamber. Samples as self-supporting disks (absorbance 0.5) were placed in a controlled-atmosphere cell for treatment. XANES spectra were taken every 15 K during a 5 K min^{-1} temperature ramp up to 673 K, in the presence of a flow of the $C_3H_6 + CO + NO + O_2$ gas mixture (as employed for catalytic activity tests). Note that XANES and DRIFTS experiments are run up to 673 K as chemical changes detected in the samples (see Section 3) are completed below such limiting temperature.

Results obtained in XANES experiments were subjected to normalization using standard procedures and analyzed using principal component analysis (PCA) [21–23] which assumes that the absorbance in a set of spectra can be mathematically modeled as a linear sum of individual components,

called factors, which correspond to each one of the palladium species present in a sample, plus noise [24]. To determine the number of individual components, an F test based on the variance associated with factor k and the summed variance associated with the pool of noise factors was performed. A factor was accepted as a "pure" chemical species (i.e., a factor associated with signal and not noise) when the percentage of significance level of the F test, %SL, was lower than a test level set in previous studies at 5%. The latter means that the null hypothesis of the F test, e.g., that factor k is associated with noise, is rejected for %SL values below such limiting value. The ratio between the reduced eigenvalues, $R(r)$, which describes the ratio between the mathematical norm of factors, was also used in determining the number of chemical species present in the sample. This ratio should approach one (e.g., equal statistical "weight") for noise-only factors. These tests are fully described in Ref. [21]. Once the number of individual components was set, XANES spectra corresponding to individual Pd species and their concentration versus temperature profiles were generated by an orthogonal rotation (varimax rotation) which should align factors (as close as possible) along the unknown concentration profiles, followed by iterative transformation factor analysis (ITFA). ITFA starts with delta function representations of the concentration profiles, associated with each chemical species, located at temperatures predicted by the varimax rotation, which are then subjected to refinement by iteration until error in the resulting concentration profiles is lower than the statistical error extracted from the set of raw spectra [21–23].

3. Results and discussion

Fig. 1 shows the isoconversion temperatures for 20 (T_{20}) and 50% (T_{50}) HC, CO, and NO conversion from the light-off curves. From the T_{20} values, representing the initial part of the light-off curves, it appears quite evident that the PdCZ system presents the lowest temperature for both oxidation reactions while differences between PdA and PdCZA were less significant. A more complex behavior was evident for the NO conversion profiles which have been analyzed in previous studies using simpler CO + NO + O_2 stoichiometric mixtures [13].

In order to test a potential relationship between the presence of a particular Pd phase and catalytic oxidation activity (particularly HC) during light off, an in situ XANES study in the presence of the complete reaction mixture was performed. The sharp deviations in the %SL and $R(r)$ values (Table 1) clearly indicate the existence of two species for PdA and PdCZA and three for PdCZ. The concentration profiles associated with these species are displayed in Fig. 2 together with the profile for PdCZ under a CO + NO + O_2 mixture (two species; dashed lines in Fig. 2). It can be seen that the maximum rate of conversion of the initially present Pd species occurs at ca. 490 K for PdCZ, 500 K for PdA,

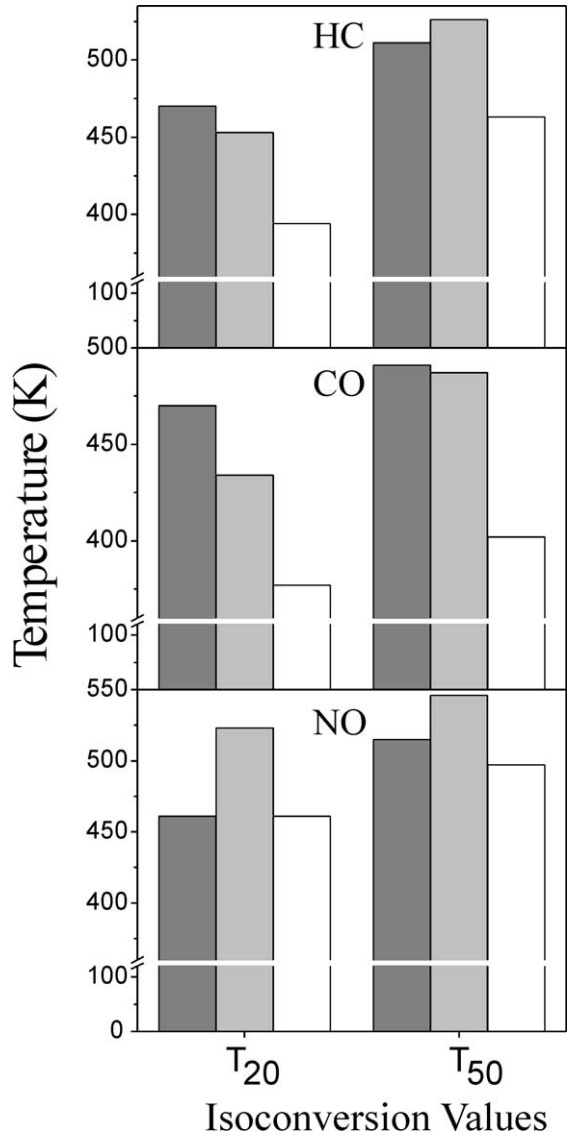

Fig. 1. Isoconversion temperatures for 20 and 50% conversion of HC, CO, and NO. Dark gray, PdA; light gray, PdCZA; and white PdCZ.

and 525 K for PdCZA. Only in the case of PdCZ was an intermediate Pd species detected. This species displayed a maximum concentration around 570 K, before conversion to a third and final Pd phase.

The XANES spectra corresponding to the chemical matrixes containing the noble metal are shown in Fig. 3. Fig. 3A displays the spectra of the initial species which may be compared with the spectrum of a PdO reference. As XANES is sensitive to local symmetry [23], this comparison indicates that Pd is initially present in an oxidic, D_{2h}-like environment for all samples. Small differences between the samples and the reference can be mostly ascribed to the small particle size, although in the case of the PdCZ it is apparent that adsorbed species from the reaction mixture may contribute to the differences. In fact, the Pd XANES spectra obtained after calcination (not shown) strongly resemble those displayed by the other samples in Fig. 3A. As a significantly lesser

Table 1
Principal component analysis of Pd K-edge XANES results

Factor	Eigenvalue	%SL	$R(r)$	Variance
		A. PdA		
1	407.35	0.00	957.34	99.897
2	0.38858	0.00	40.32	0.095
3	0.00875	20.09	1.32	0.002
4	0.00596	24.38	1.37	0.002
5	0.00387	31.19	1.01	0.001
6	0.00243	30.94	1.21	
7	0.00224	35.92	0.93	
8	0.00157	34.58	1.20	
		B. PdCZA		
1	490.42	0.00	1453.4	99.935
2	0.31265	0.00	105.32	0.064
3	0.00273	8.04	1.44	
4	0.00174	8.79	1.73	
5	0.00090	14.61	1.75	
6	0.00047	24.05	1.59	
7	0.00026	34.86	0.97	
8	0.00023	34.56	1.17	
		C. PdCZ		
1	475.72	0.00	911.32	99.893
2	0.48109	0.00	17.43	0.101
3	0.02541	0.00	16.73	0.005
4	0.00139	10.67	1.64	
5	0.00076	16.38	2.08	
6	0.00033	32.14	0.99	
7	0.00030	31.81	1.16	
8	0.00022	35.84	0.99	

Variances lower than 10^{-3} are not reported.

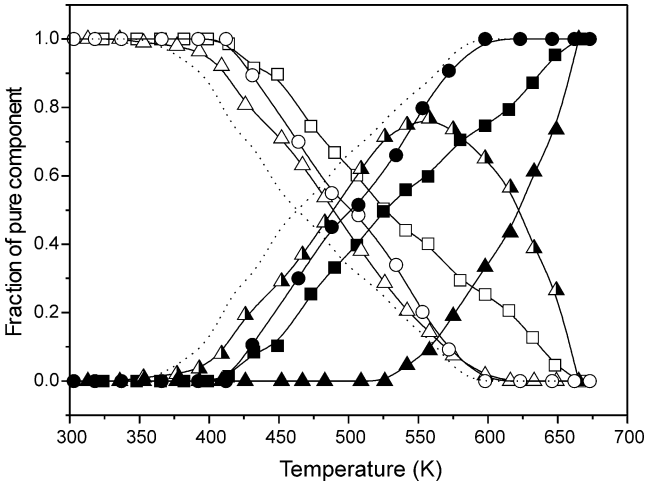

Fig. 2. Concentration profiles during the temperature-programmed reaction run for Pd-containing species. Initial species (open symbols); intermediate species (half-filled symbols), and final species (filled symbols). Circles, PdA; squares, PdCZA; triangles, PdCZ; dashed lines, profiles of the PdCZ species under a $CO + NO + O_2$ reaction run.

perturbed spectrum of the initial Pd species of PdCZ was obtained under a $CO + NO + O_2$ reaction mixture (Fig. 3C), it may be deduced that the shape of the XANES spectrum for PdCZ is influenced by the presence of propene even at room temperature. The analysis of DRIFTS spectra of PdCZA

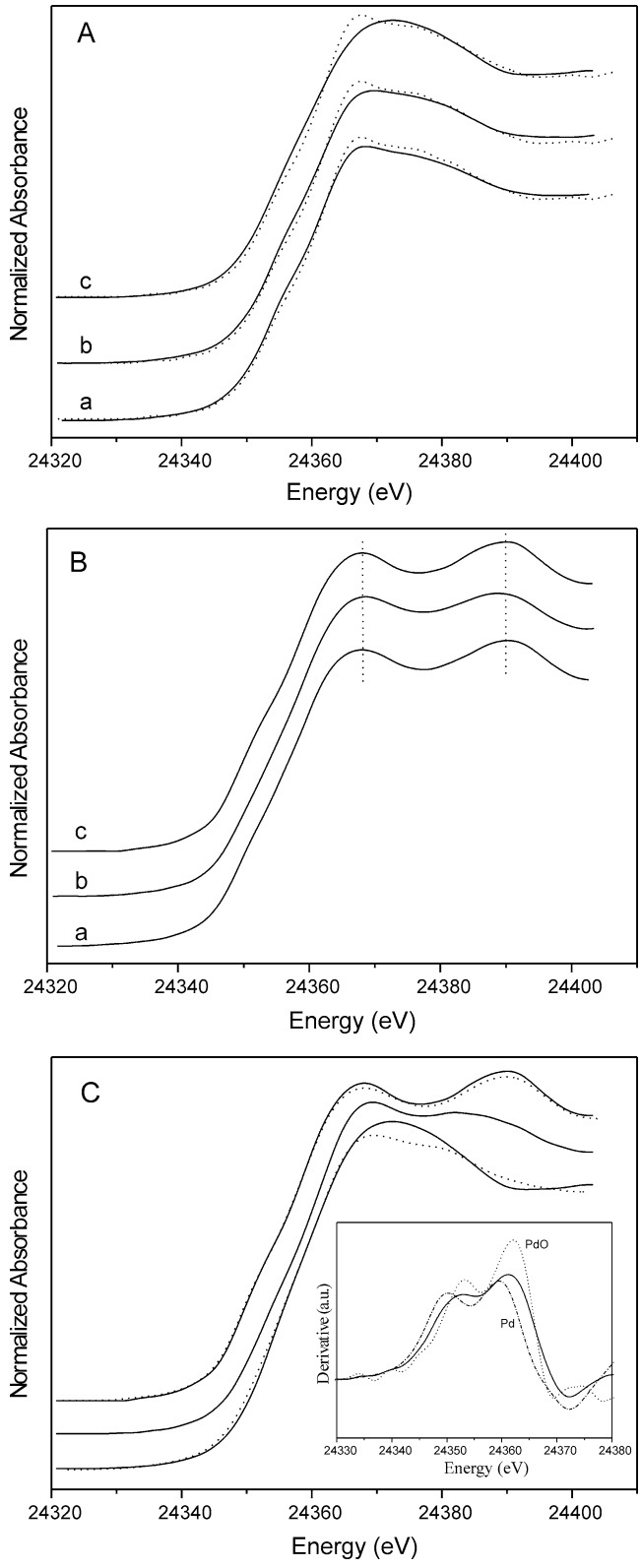

Fig. 3. XANES spectra for PCA predicted chemical species. (A) Pd initial, oxidized species; (B) Pd final, reduced species; and (C) Pd species detected for the PdCZ sample; lower, initial; middle, intermediate; upper, final species. Full lines, Pd species under $C_3H_6 + CO + NO + O_2$; dashed lines, PdO (A) and Pd species under $CO + NO + O_2$ (C). Inset in (C) shows derivative spectra of the Pd intermediate species and reference compounds. Lower case labels (a) PdA, (b) PdCZA, and (c) PdCZ.

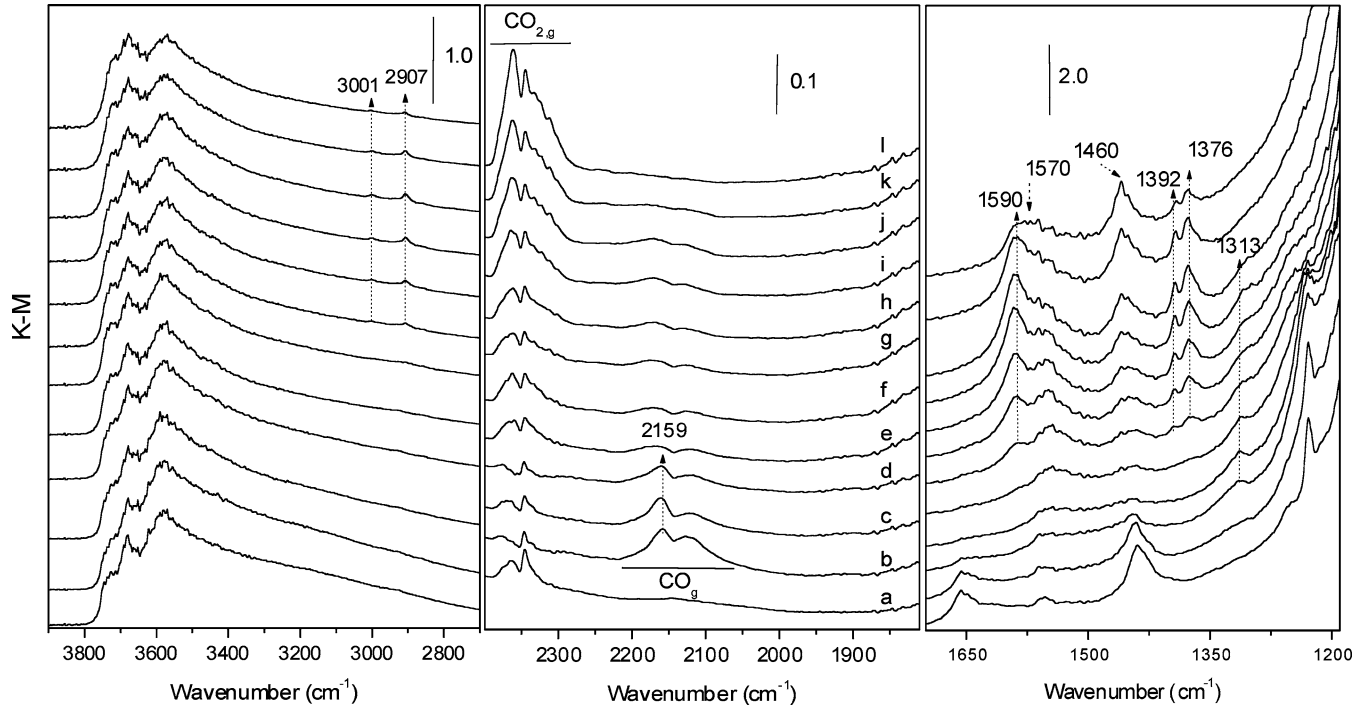

Fig. 4. DRIFTS spectra of PdCZA, sample in a flow of N_2 at 303 K (a) and 0.1% C_3H_6, 1% CO, 0.9% O_2, 0.1% NO, N_2 balance at (b) 303, (c) 348, (d) 378, (e) 423, (f) 453, (g) 483, (h) 503, (i) 523, (j) 553, (k) 608, and (l) 653 K.

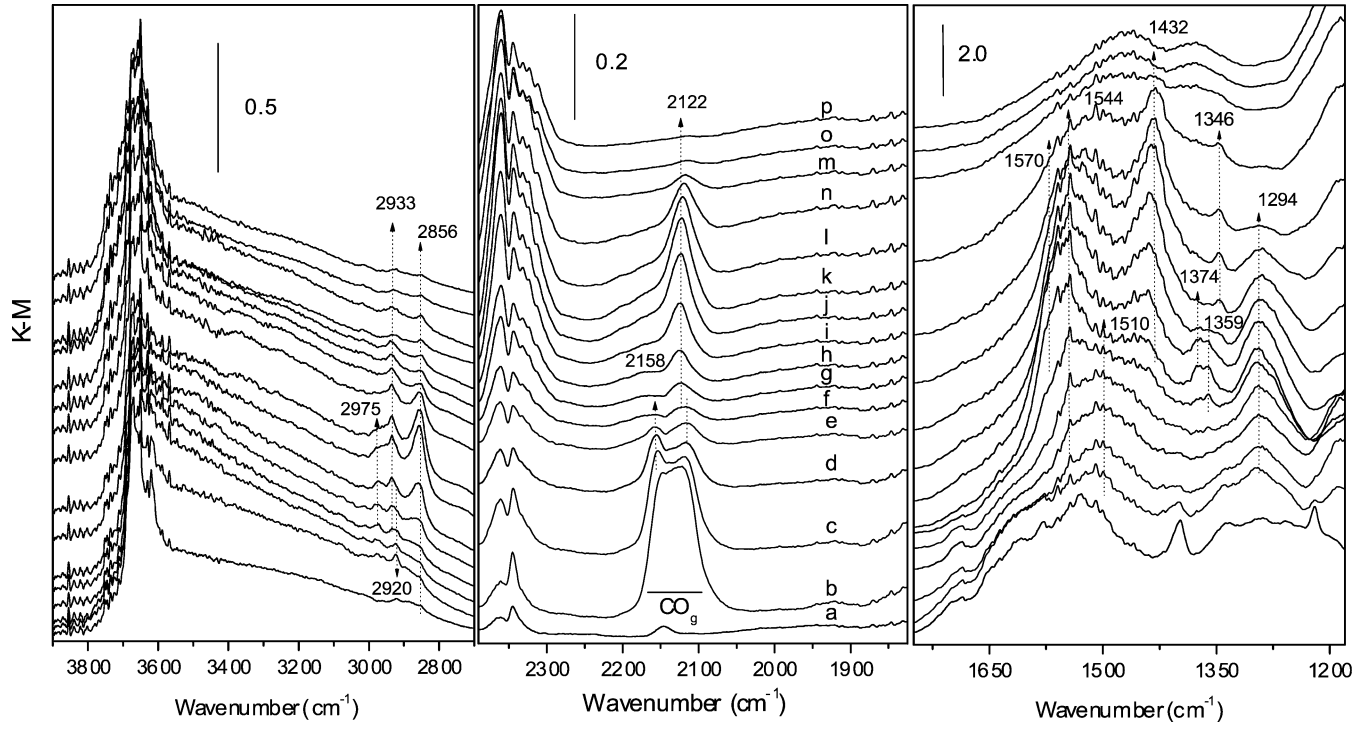

Fig. 5. DRIFTS spectra of PdCZ, sample in a flow of N_2 at 303 K (a) and 0.1% C_3H_6, 1% CO, 0.9% O_2, 0.1% NO, N_2 balance at (b) 303, (c) 363, (d) 393, (e) 408, (f) 423, (g) 453, (h) 483, (i) 513, (j) 543, (k) 573, (l) 603, (n) 633, (m) 663, (o) 693, and (p) 723 K.

(Fig. 4) and PdCZ (Fig. 5) taken during a light-off test in fact shows that the HC is able to strongly interact with the PdCZ system but not with PdCZA. Thus, Fig. 5 display several C–H vibration modes ($\gamma_{as}/\gamma_s(CH_2)$ 2933/2856 cm^{-1}; $\gamma_{as}/\gamma_s(CH_3)$ 2975/ $\approx$ 2870 cm^{-1}), indicative of the presence of saturated hydrocarbon chains adsorbed on ceria-containing surfaces [25], already from very low temperatures. As the thermal behavior of such bands does not cor-

relate with that of bands appearing in the 1800–1200 cm^{-1} region and potentially ascribable to γ_{as}/γ_s(OCO) or γ(CO) modes, it is likely that propene interaction with PdCZ induces formation of polymeric (and not carbonyl- or carboxylate-type) species. These polymeric species are not detected with the support alone (result not shown) and must be formed by propene interaction with the noble metal; the XANES analysis (Fig. 3C) indicates that a π-complex of propene (or propene-derived) species and fully oxidized Pd(II) is likely involved in the initial step of such interaction. Important to stress is the fact that such polymeric adsorbate(s) as well as Pd(II) species influenced by the reactive mixture are not observed for the PdCZA system (Figs. 3 and 4), although contact between the noble metal and the promoter exists in this sample [20]. Therefore, it can be concluded that the presence of CZ tridimensional patches is needed to facilitate the activation of the HC at low temperatures.

On the other hand, the initially present Pd species were converted to Pd(0) particles for all samples (Fig. 3B) with the latter appearing at similar temperatures (above 423 K) for PdA and PdCZA while for PdCZ the metallic species was only detected above 550 K (Fig. 2). For the latter sample, comparison with the evolution of Pd species under the $CO + NO + O_2$ reaction mixture shows that Pd(0) appeared at much lower temperatures (above 373 K; dashed lines in Fig. 2) in the absence of the hydrocarbon, again indicating a significant role played by propene in the behavior of Pd for this sample. The XANES spectrum of the intermediate Pd state during the reduction of the PdCZ catalyst is presented in Fig. 3C together with the reduced and oxidized reference Pd species. Analysis of the derivative of the absorption edge region of the Pd intermediate (inset Fig. 3C) clearly shows a small shift, half-way between the Pd metal and the PdO references, but having a rather similar shape to the oxidized compound. Further differences between the spectrum of the intermediate Pd state and the PdO reference can be appreciated in the continuum region, with the presence of a continuum resonance (CR) at about 24,385 eV, absent in PdO. This CR is associated with (the $l = 1$ projection of) 4f Pd-like states [23] and is therefore indicative of the presence of Pd–Pd contacts at distances much closer than those in PdO and also of a certain, limited (probably a 1D or 2D conductor as in some Pd(I) oxides; see Ref. [26]) metallic-like character. An alternative to the Pd–Pd contact would involve a Pd–Ce(Zr) interaction but the proximity of the 4f Ce levels to the Fermi edge [27,28] would produce distinctive features (CRs) not present in our XANES spectrum. In summarizing all these data, the intermediate Pd species can be described as a Pd cluster with an average Pd^{n+} (n close to 1) oxidation state, likely induced by the presence of oxygen in the network, but having a certain metallic-like character derived from the existence of Pd–Pd chemical bonds. The strong interaction with propene-derived (polymeric) ad species, already detected for the Pd(II) state (Figs. 3A–C), is necessary in generating this Pd(I)-like species and can be interpreted as being stabilized by such surface CH_x entities. It should be noted that the possibility of a well-formed Pd carbide phase is dismissed as the corresponding Pd K-edge XANES shape of such a phase would resemble that of the zero-valent, metallic system, with small red shifts in the CR positions [29].

The presence of the Pd intermediate state at the catalytically active surface of the material is demonstrated by DRIFTS. The middle panel of Fig. 4 displays PdCZA DRIFTS spectra in the C–O-stretching region during a reaction run. No significant differences were encountered when analyzing the behavior of the PdA (result not shown). The band at 2159 cm^{-1} shows evidence of CO adsorbed at Pd(II) sites [13,30,31], visible over the doublet characteristic of CO_g. Such ad species were also detected for PdCZ (Fig. 4) up to a similar temperature (ca. 393 K) but above 333 K, these coexist with a Pd(I)-like carbonyl, responsible for the 2115–2122 cm^{-1} band [13,30,31]. All these bands are generated by adsorption of CO from the gas phase. Initially, at the lowest temperature (Fig. 5b), the band due to surface Pd(I)-like carbonyls displayed a greater intensity than that of Pd(II) carbonyls but this is somewhat expected due to the larger extinction coefficient of the stronger covalent-like CO interaction with a Pd species with some metallic character [32] with respect to the more labile character of a Pd(II)–CO bond. The 2115–2122 cm^{-1} band was still apparent up to 693 K (Fig. 5m), indeed indicating the formation of a strong Pd–adsorbate bond. The intensity of this band displayed, however, an unusual behavior; it decreased up to 423 K before gaining intensity above such a temperature. As will be shown elsewhere [33], analysis of the $CO + NO + O_2$, $C_3H_6 + O_2$, and $C_3H_6 + NO$ reactions allows us to correlate the carbonyl intensity increase with the onset of the NO reduction process (using hydrocarbon as reductant) which gives CO as a by-product, and thus increases the CO_g concentration near the Pd particles. On the other hand, the presence of surface Pd(I)-like species (Fig. 5) is concomitant with the temperature region in which the Pd intermediate species was detected by XANES (Fig. 2) and may thus be considered as the dominant Pd surface state associated with the Pd intermediate phase. Note that CO adsorbed species are not involved in the stabilization of the Pd(I)-like phase, as demonstrated by the absence of such a phase in similar XANES experiments under a $CO + NO + O_2$ mixture (Figs. 2 and 3C).

To conclude, the XANES/DRIFTS study gives evidence of the influence of the support in the manner in which the distinct Pd species evolve with reaction temperature. Contact between Pd and the bare alumina surface (PdA) or with two-dimensional patches of the CZ component (PdCZA) [13] gives rise to negligible differences in the onset temperature for conversion of the PdO phase at around 423 K. In the case of PdCZ, on the other hand, conversion of this phase begins at a lower temperature (ca. 373 K) and, more importantly, yields a partially oxidized Pd species which, may, however, possess enough metallic-like character to activate

the hydrocarbon at "low temperatures" (below 473 K). As noted above, the availability of oxygen anions from the Pd phase may correlate with the initial HC light-off temperature [15,16]. The presence of the Pd(I)-like intermediate for the PdCZ, as detected by XANES and DRIFTS, can be associated with the lowering of the latter parameter (see T_{20} values in Fig. 1) when comparing the three catalysts. The contact between Pd and tridimensional CZ patches stabilizes the intermediate Pd phase between 373 and 673 K, a temperature range which may easily cover those reached during the cold start of gasoline engines and thus may open a pathway to decrease HC emissions in gasoline-fueled vehicles. The intermediate Pd(I)-like phase is also observed in the second light-off run for the PdCZ system but significant changes in the temperature range of existence and properties of the active phase are detected and are currently investigated. Further studies of the nature, stability, and physicochemical properties of this phase after aging treatments, under lambda oscillations and, particularly, net reducing conditions, are needed to definitively set the importance of this phase in the elimination of HC during cold start. On the other hand, this hydrocarbon-mediated stabilization mechanism of a (partially) oxidized Pd state appears inherent to a CZ-supported system and can be compared with the recently reported stabilization mechanism of Pd into solid solutions with a perovskite-type structure [34].

Acknowledgments

We thank the Comunidad de Madrid for grants received (to A.B.H. and A.I.-J.) with which this work has been carried out and for financial assistance (to A.B.H.) under the "Ayudas para estancias breves en centros de investigación extranjeros" program. We are also grateful to the scientific and technical staff at the ESRF Synchrotron (BM29; Dr. G. Subias) for their help during the XANES experiments. Financial help by CICYT (Project MAT2000-1467) is also acknowledged.

References

[1] E.S.J. Lox, B.H. Engler, in: G. Ertl, H. Knözinger, J. Weitkamp (Eds.), Environmental Catalysis, Wiley–VCH, New York, 1999, p. 1.
[2] A. Trovarelli, Catal. Rev. Sci. Eng. 38 (1996) 97, and references therein.
[3] R.M. Heck, R. Farrauto, Catalytic Air Pollution Control, Wiley–Interscience, New York, 2002, Chaps. 6 and 12.
[4] R. van Yperen, D. Lindner, L. Mubmann, E.S. Lox, T. Kreuzer, Stud. Surf. Sci. Catal. 116 (1998) 51.
[5] D.S. Lafyatis, G.P. Ansell, S.C. Bennett, J.C. Frost, P.J. Millington, R.R. Rajaram, A.P. Walker, T.H. Ballinger, Appl. Catal. B 18 (1998) 123.
[6] J. Kašpar, P. Fornasiero, M. Graziani, Catal. Today 50 (1999) 351.
[7] Y. Nagai, T. Yamamoto, T. Tanaka, S. Yoshida, T. Nonaka, T. Okamoto, A. Suda, M. Sugira, Catal. Today 74 (2002) 225.
[8] A. Martínez-Arias, M. Fernández-García, V. Ballesteros, L.N. Salamanca, C. Otero, J.C. Conesa, J. Soria, Langmuir 15 (1999) 4796.
[9] M. Fernández-García, A. Martínez-Arias, A. Iglesias-Juez, C. Belver, A.B. Hungría, J.C. Conesa, J. Soria, J. Catal. 194 (2000) 385.
[10] Z. Hu, C.Z. Wan, Y.K. Lui, J. Dettling, J.J. Steger, Catal. Today 30 (1996) 83.
[11] M. Skoglundh, H. Johansson, L. Löwendahl, K. Jansson, L. Dahl, B. Hirschauer, Appl. Catal. B 7 (1996) 299.
[12] J.C. Jiang, X.Q. Pan, G.W. Graham, R.W. McCabe, J. Schwank, Catal. Lett. 53 (1998) 37.
[13] A. Martínez-Arias, M. Fernández-García, A. Iglesias-Juez, A.B. Hungría, J.A. Anderson, J.C. Conesa, J. Soria, Appl. Catal. B 31 (2001) 51.
[14] Y.-F. Yu-Yao, Ind. Eng. Chem. Process Res. Dev. 19 (1980) 295.
[15] M. Shelef, G.W. Graham, R.W. McCabe, in: A. Trovarelli (Ed.), Catalysis by Ceria and Related Materials, Imperial College Press, London, 2002, pp. 368–370, Chap. 10.
[16] G.Z. Rienacker, Anorg. Alleg. Chem. 59 (1949) 280.
[17] J.Z. Shyu, K. Otto, W.L.H. Watkins, G.W. Graham, R.K. Belitz, H.S. Gandhi, J. Catal. 144 (1988) 23.
[18] M.-F. Luo, X.-M. Zheng, Appl. Catal. A 189 (1999) 15.
[19] A. Martínez-Arias, M. Fernández-García, A. Iglesias-Juez, A.B. Hungría, K. Duncan, R. Smith, J.A. Anderson, J.C. Conesa, J. Soria, J. Catal. 204 (2001) 238.
[20] M. Fernández-García, A. Martínez-Arias, A. Iglesias-Juez, A.B. Hungría, J.A. Anderson, J.C. Conesa, J. Soria, Appl. Catal. B 31 (2001) 39.
[21] M. Fernández-García, C. Márquez-Alvarez, G.L. Haller, J. Phys. Chem. 99 (1995) 12565.
[22] C. Márquez-Alvarez, I. Rodríguez-Ramos, A. Guerrero-Ruiz, G.L. Haller, M. Fernández-García, J. Am. Chem. Soc. 119 (1997) 2905.
[23] M. Fernández-García, Catal. Rev. Sci. Eng. 44 (2002) 59.
[24] E.R. Malinowsky, Factor Analysis in Chemistry, Wiley, New York, 1991.
[25] A. Yeo, S.J. Morisson, H. Idriss, J. Catal. 186 (1999) 279, and references therein.
[26] R.D. Shannon, D.B. Rogers, C.T. Prewitt, Inorg. Chem. 10 (1971) 713.
[27] A. Vega, S. Bouarab, M.A. Khan, Phys. Rev. B 51 (1995) 4823.
[28] W. Scheider, S.L. Molodtsov, M. Ritcher, Th. Gantz, P. Engelmenn, C. Lauschat, Phys. Rev. B 57 (1998) 14930.
[29] J.A. McCaulley, Phys. Rev. B 47 (1983) 4873.
[30] A. Bensalem, J.C. Muller, D. Tessier, F. Bozon-Verduraz, J. Chem. Soc., Faraday Trans. 92 (1996) 3233.
[31] M. Fernández-García, A. Martínez-Arias, L.N. Salamanca, J.M. Coronado, J.A. Anderson, J.C. Conesa, J. Soria, J. Catal. 187 (1999) 474.
[32] F. Illas, N. Lopez, J.M. Ricart, A. Clotet, J.C. Conesa, M. Fernández-García, J. Phys. Chem. B 102 (1998) 8017.
[33] M. Fernández-García, unpublished results.
[34] H. Tanaka, I. Tan, M. Uenishi, M. Kimura, K. Dohmae, Top. Catal. 16/17 (2001) 63.